TÜBİTAK

Turkish Journal of Earth Sciences

http://journals.tubitak.gov.tr/earth/

Research Article

Turkish J Earth Sci
(2014) 23: 479-494

doi:10.3906/yer-1401-23

A 3D model for the formation of turtleback surfaces: the Horzum Turtleback of western Turkey as a case study

Gürol SEYİTOĞLU*, Veysel IŞIK, Korhan ESAT
Department of Geological Engineering, Tectonics Research Group, Ankara University, Tandoğan, Ankara, Turkey

Received: 17.01.2014 • **Accepted:** 01.07.2014 • **Published Online:** 01.09.2014 • **Printed:** 30.09.2014

Abstract: Turtleback surfaces are common elements of highly extended terrains all over the world. This paper presents a 3D model explaining the formation of turtleback surfaces based on field observations made on the Horzum Turtleback of the Alaşehir graben, western Turkey. Three essential features have been determined as forming a turtleback surface. These are 1) the rolling hinge mechanism on a normal fault system, where the initial fault stays operational after forming second and third normal faults in its hanging wall; 2) relay ramps between initial fault segments; and 3) a synextensional intrusion on the shear zone of the initial normal fault at midcrustal level. The strike-slip tectonic setting is not among the essential features as suggested recently for Death Valley turtlebacks.

Key words: Turtleback, extension, normal fault, Death Valley, western Turkey, graben

1. Introduction

The term 'turtleback' was introduced to the geological literature by Curry (1938, 1949) and had a morphological meaning that determined surfaces similar to the carapace of turtles. The origins and formation mechanisms of turtleback surfaces have been debated since then. Curry (1949, 1954) described the Badwater, Copper Canyon, and Mormon Point turtlebacks of Death Valley, USA (Figure 1), and suggested that these structures were related to thrust faulting. Drewes (1959), on the other hand, evaluated the turtlebacks as postfolded erosional features with normal faults playing an important role in their exhumation. Strike-slip–related contraction (Hill and Troxel, 1966) and strike-slip–related normal faulting (Wright et al., 1974) are among other suggested mechanisms for turtleback surfaces. After recognition of the metamorphic core complexes and low-angle normal faults in the Basin and Range Province (Davis, 1980; Rehrig and Reynolds, 1980; Wernicke, 1981), the Death Valley turtlebacks have been evaluated as part of a regional detachment surface (Stewart, 1983). This was the beginning of a long debate about the role of low-angle vs. deep-seated normal faulting in the formation of turtlebacks (Wernicke et al., 1988; Miller, 1991; Holm et al., 1994; Miller and Prave, 2002; Miller and Pavlis, 2005). Isotopic age data and paleomagnetic studies have broadened understandings of the Death Valley geology. Holm et al. (1992) provide $^{40}Ar/^{39}Ar$ biotite ages (13–6.7 Ma) from the turtlebacks indicating a midcrustal origin prior to the extension and exhumed by the rolling hinge mechanism. Paleomagnetic data demonstrate a 50° to 80° clockwise vertical axis rotation since 8.7 Ma in the Death Valley region. This rotation has been attributed to a right lateral shearing (Holm et al., 1993). Miller and Pavlis (2005) gave an outstanding review of the earlier works and concluded that multiple faults, rather than a single detachment fault, play an important role in the development of the turtlebacks. Most recently, Norton (2011) suggested that the turtlebacks are megamullions formed by the strike-slip faulting in the Death Valley area and that these structures are unique to the western North America extensional province. Most earlier attempts to explain the turtleback formation are 2D models drawn on a cross-sectional view. The 3D model presented here is based on field observations of the Horzum Turtleback (Çemen et al., 2005) at the southern flank of the Alaşehir graben in western Turkey, where no major strike-slip faulting is reported (Figure 2). For this reason, this 3D model could also be useful in the evaluation of the Death Valley turtlebacks that have a relatively more complex structural history (i.e. Basin and Range extension plus strike-slip shearing; see Norton, 2011).

2. Geological setting of the Alaşehir graben, western Turkey

Western Turkey is located on the eastern part of the Aegean extensional province, having the Menderes massif surrounded by the İzmir-Ankara Suture Zone and Lycian

* Correspondence: seyitoglu@ankara.edu.tr

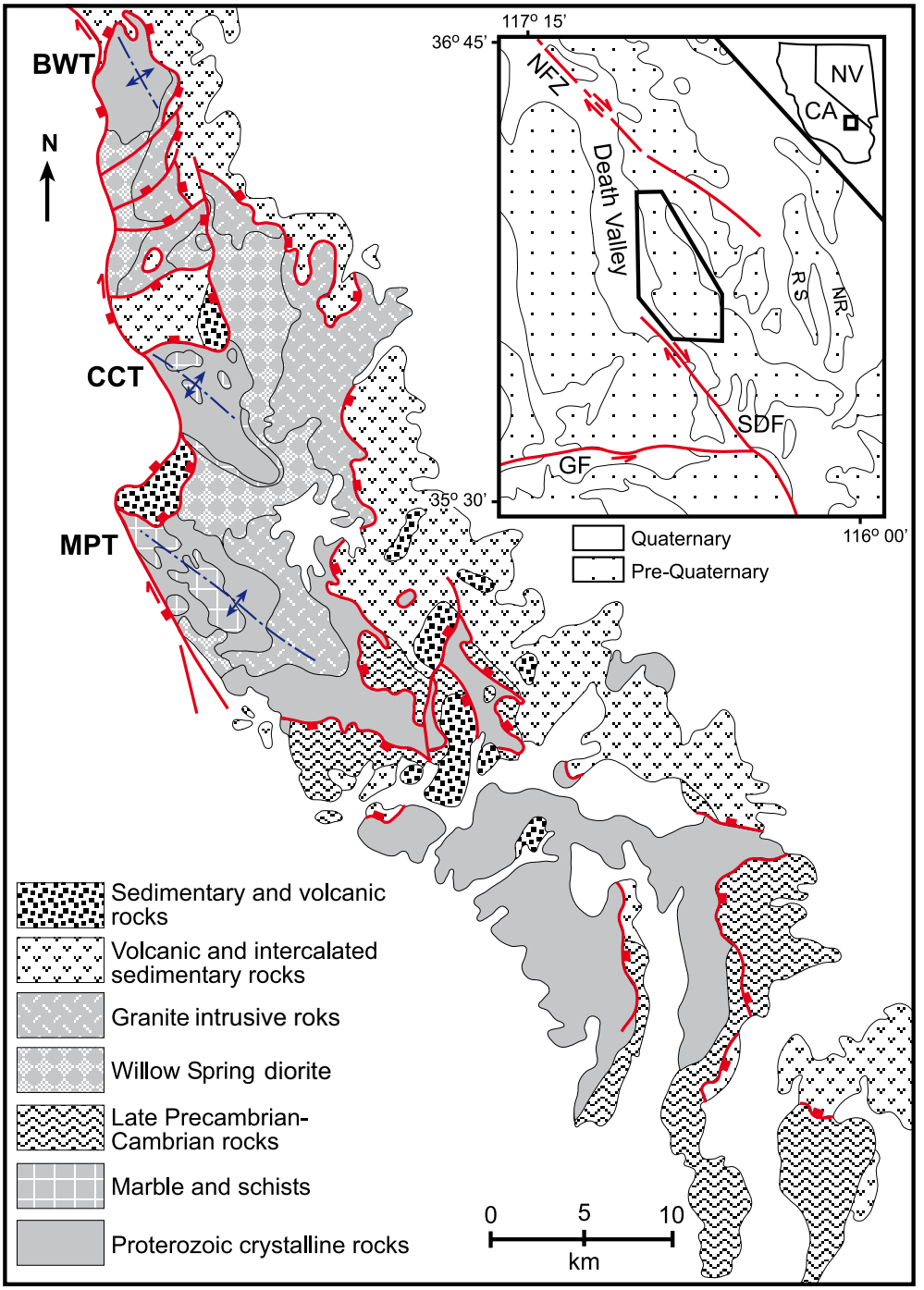

Figure 1. Geological map of Black Mountains (after Holm and Wernicke, 1990). NV: Nevada, CA: California, NR: Nopah Range, RS: Resting Springs, NFZ: Northern Death Valley-Furnace Creek Fault Zone, SDF: Southern Death Valley Fault Zone, GF: Garlock Fault, BWT: Badwater Turtleback, CCT: Copper Canyon Turtleback, MPT: Mormon Point Turtleback.

nappes from the north and south, respectively (Figure 2a). The Menderes massif has an elliptical shape with a NE-SW–trending long axis and it is traditionally defined as a Precambrian gneissic core with Paleozoic–Early Tertiary metasedimentary cover rocks separated by an unconformity (Şengör et al., 1984; Candan et al., 2011). Recent studies demonstrate that the Menderes massif can be regarded as a core complex called the Menderes Core Complex

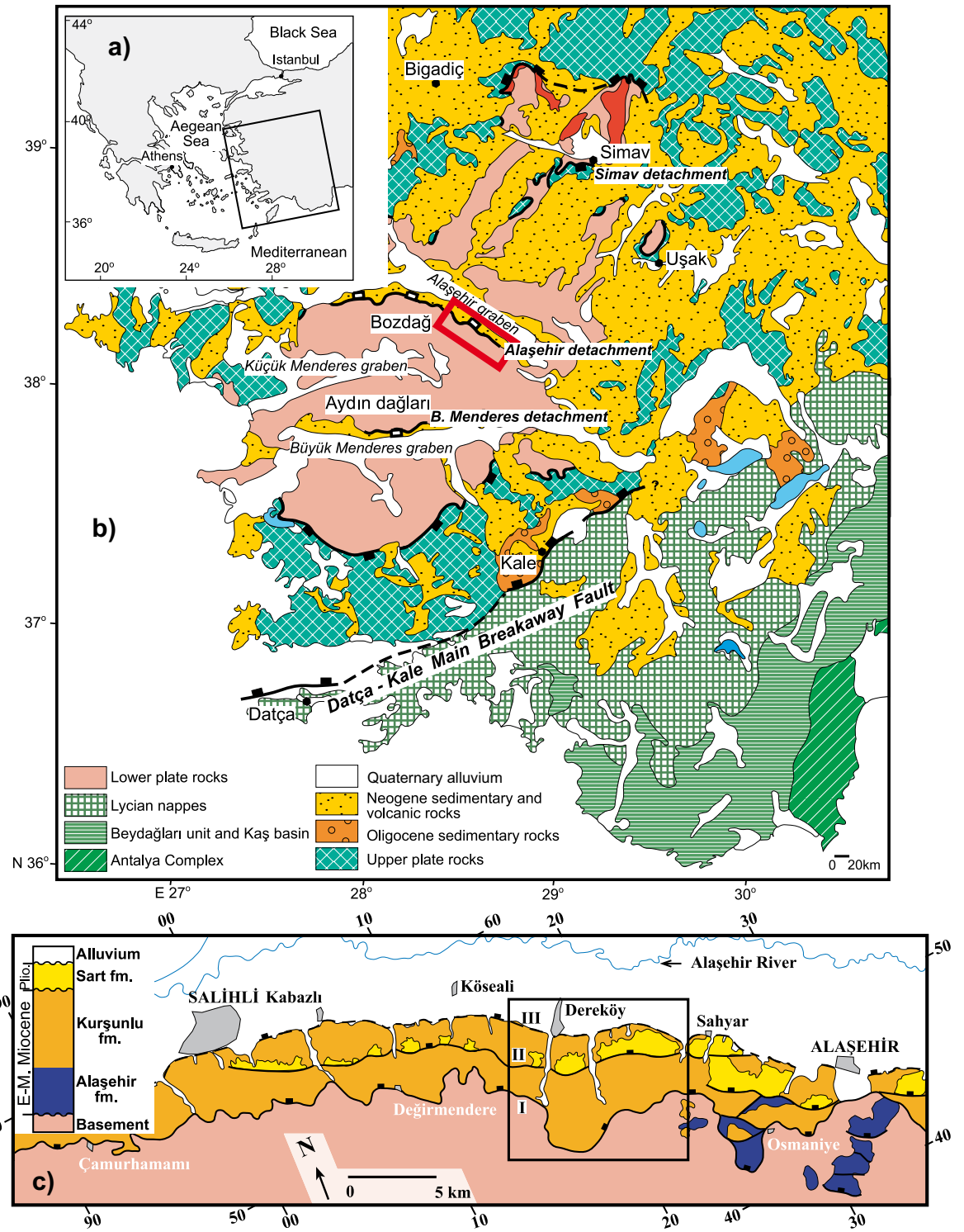

Figure 2. a) Location of western Turkey in the east of the Aegean Region. **b)** The main tectonic elements of western Turkey (after Seyitoğlu et al., 2004). **c)** Geological map of the Alaşehir Graben (after Seyitoğlu et al., 2000).

(MCC) (Bozkurt and Park, 1994; Gessner et al., 2001; Işık and Tekeli, 2001; Ring et al., 2003; Seyitoğlu et al., 2004). Several detachment faults and/or related shear zones that controlled the exhumation of the Menderes massif have been described and mapped (e.g., Işık et al., 2003, 2004). The lower plate rocks of the MCC contain mainly gneisses

(para-gneiss, orto-gneiss) and high-grade mica schists. Lesser amounts of amphibolite (metagabbro, eclogite), quartzite, and marble are also found. Its upper plate rocks are composed of non- and low-grade metamorphic rocks, ophiolitic rocks, and Tertiary sedimentary units. The complete exhumation history of the MCC has been discussed in recent review papers (i.e. ten Veen et al., 2009; Hinsbergen, 2010); there are 2 main models. In the symmetrical exhumation model, the Menderes massif was exhumed along the south-dipping Lycian detachment and north-dipping Simav detachment (Ring et al., 2003). In the asymmetrical model, however, the exhumation of the Menderes massif occurred along the north-dipping Datça-Kale main breakaway fault and its northern continuation, the Simav detachment, during the Oligocene (Seyitoğlu et al., 2004). Both models agree that the central Menderes massif was further exhumed along the bivergent Alaşehir and Büyük Menderes detachment faults bounding the southern and northern sides of the Alaşehir and Büyük Menderes grabens, respectively (Figures 2b and 2c). Although many different interpretations of the formation of the grabens exist (Koçyiğit et al., 1999; Yılmaz et al., 2000; Yılmaz and Gelişli, 2003; Bozkurt and Sözbilir, 2004; Purvis and Robertson, 2005; Gürer et al., 2009; Çiftçi and Bozkurt, 2010; Öner et al., 2010; Öner and Dilek, 2011), the development of the grabens is well explained by the rolling hinge mechanism (Seyitoğlu and Şen, 1998; Gessner et al., 2001; Seyitoğlu et al., 2002; Demircioğlu et al., 2010) (Figure 3).

In the initial development of the Alaşehir graben, the high-angle normal faults (Fault I) controlled the deposition of first and second sedimentary units (Alaşehir and Kurşunlu Formations) during the Early Miocene (Seyitoğlu et al., 2002) (Figures 2c and 3a). Both units have an Eskihisar sporomorph association (20–14 Ma) (Ediger et al., 1996; Seyitoğlu and Scott, 1996). Moreover, the transition from the first to the second sedimentary unit has been dated by magnetostratigraphy (16.6–14.6 Ma; Şen and Seyitoğlu, 2009). At the same time, in the midcrust, the synextensional Salihli granitoid intruded into the ductile shear zone of Fault I (15 Ma; Glodny and Hetzel, 2007).

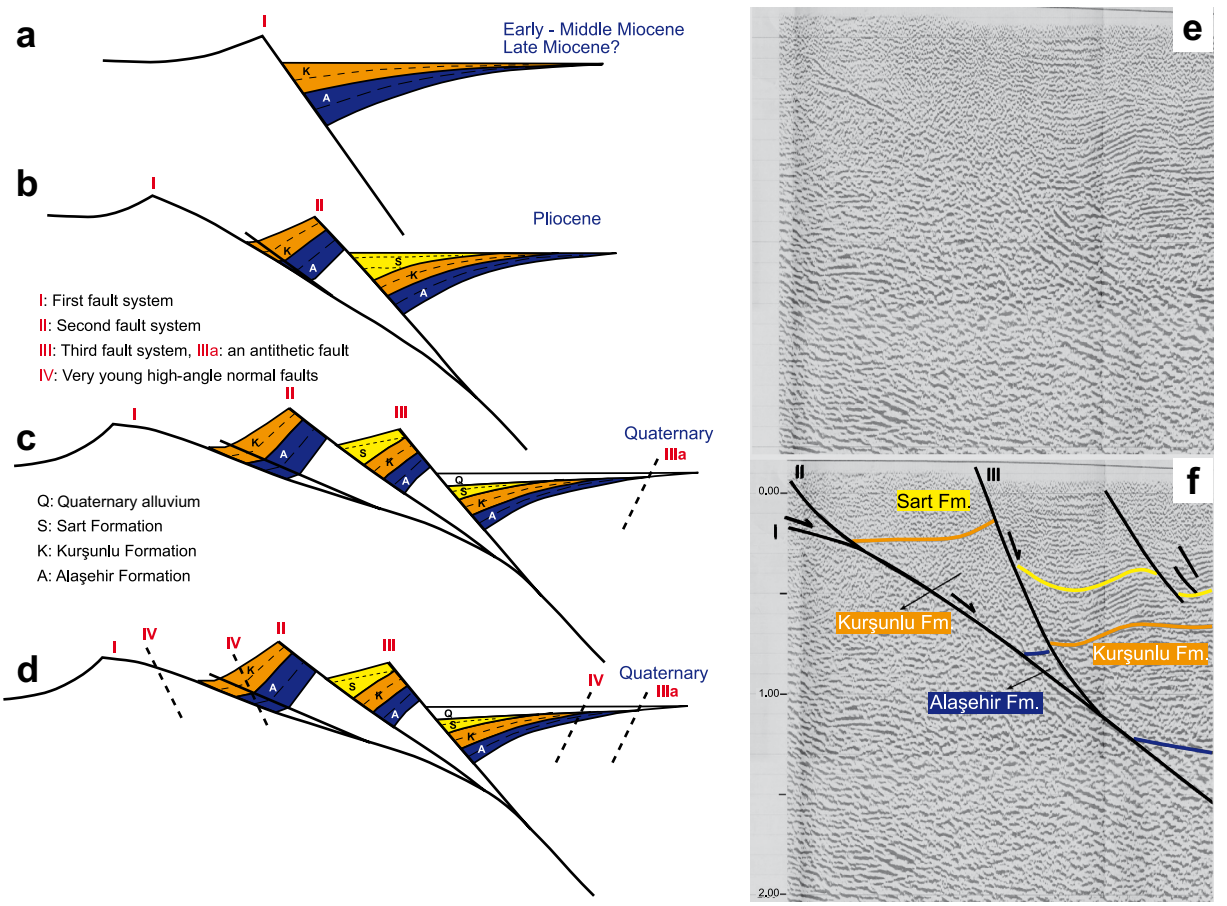

Figure 3. a–d) Suggested rolling hinge mechanism for the Alaşehir graben (after Seyitoğlu et al., 2002). **e, f)** Enlarged seismic section shows the evidence of merging faults at the subsurface (after Demircioğlu et al., 2010).

In the Pliocene, Fault II developed in the hanging wall of Fault I and it controls the deposition of the third sedimentary unit (Sart Formation) (Figures 2c and 3b). Fault I rotated to the back and was getting a low angle, similar to the rolling hinge mechanism (Buck, 1988; Wernicke and Axen, 1988). As pointed out by Seyitoğlu et al. (2002, p. 23), Fault I, gaining shallower angles, is also active along with Fault II, proven by the parallel shear zones in the second sedimentary unit. The samples from same location are dated as 9.2 ± 0.3 Ma and 3.7 ± 0.2 Ma (Hetzel et al., 2013, samples 10Me09 and 10Me10). The rock units between Fault I and II reside in a simple shear zone where a progressive deformation is possible (Şengör and Bozkurt, 2013).

In the Quaternary, Fault III appeared in the hanging wall of Fault II and led to the further rotation of Fault I and II. In the hanging wall of Fault III, Quaternary alluvium deposits have accumulated. By developing antithetic normal faults on the northern side, the graben has become symmetrical (Figure 3c). In the Quaternary-recent period, Fault IV chopped the earlier structures (Figure 3d) (Seyitoğlu et al., 2002). These youngest structures do not affect the earlier rolling hinge mechanism in the Alaşehir graben, as is proven by seismic data showing that Faults II and III nicely merge to Fault I, today's low-angle detachment fault on the southern flank of the Alaşehir graben (Figures 3e and 3f) (Demircioğlu et al., 2010) where the Horzum Turtleback (Çemen et al., 2005) was determined (Figure 4).

3. Evaluation of isotopic dating on the Alaşehir detachment

The southern margin of the Alaşehir graben is limited by the Alaşehir detachment fault. The Alaşehir detachment fault is a regional-scale, low-angle normal fault that trends approximately E-W and dips about 10°–30° (Işık et al., 2003) with a well-developed shear zone. The footwall of the Alaşehir detachment fault is composed of medium- to high-grade metamorphic rocks (garnet mica schist/gneiss, kyanite staurolite garnet mica gneiss, calc-silicatic schist/gneiss, amphibolite) and syntectonic granitoid intrusions (Figure 4) (Hetzel et al., 1995; Işık et al., 2003; Glodny and Hetzel, 2007; Öner et al., 2010). The rocks along the Alaşehir detachment underwent mylonitization during the early stages of extensional ductile deformation with a top to north-northeast sense of shearing and this was overprinted by brittle deformation at later stages, which indicates a ductile to brittle transition (Işık et al., 2003) (Figures 2c and 4). A locally protected slickenside on the Alaşehir detachment includes slickenlines that can be compared with mylonitic lineations within the mylonites along the Alaşehir shear zone, suggesting that both ductile and deformation structures occurred under the same extensional regime (Işık et al., 2003).

There are considerable isotopic data yielded from both fault rocks and the protolith of the fault rocks along the Alaşehir detachment, and it is one of the intensively dated fault surfaces on earth. A large variety of the age results, ranging from 1.75 ± 0.62 Ma to 21.70 ± 4.50 Ma (see the Table and references), are obtained by the different methods. We have plotted all available isotopic age data from the Alaşehir detachment to a cross-section by using elliptical trajectories (Table; Figures 5 and 6), because simple latitude values of the samples may not reflect the real positions in respect to the overall fault surface.

The rolling hinge model suggested to explain the Alaşehir graben's evolution (Seyitoğlu et al., 2002) is different than the original model (Buck, 1988; Wernicke and Axen, 1988). While the original model proposes an inactive, rotated initial fault, the model suggested for the Alaşehir graben indicates an active, rotated initial fault, based on field observations (Alaşehir type rolling hinge model; Seyitoğlu et al., 2002, p. 24). This view is supported by recently published isotopic dating on the Alaşehir detachment where the results are scattered irrespective of their location and method (Table; Figure 6). In other words, the results are opposite to the case of an inactive rotated initial fault of the original rolling hinge mechanism, for which an age distribution on a rotated fault getting older towards the south would be expected.

All available isotopic age data indicate that Fault I, active at least in 3 different time intervals, played an important role in the formation of the Horzum Turtleback surface in the Alaşehir graben. The earliest time interval is 20–15 Ma (Figure 6), corresponding to the accumulation of the Alaşehir and Kurşunlu Formations in the hanging wall of the high-angle Fault I. The second time interval is between 10 and 5 Ma, matching the formation of Fault II and the accumulation of the Sart Formation in its hanging wall. Fault I starts to rotate to lower angles and shearing also occurs in this position. The third time interval is younger than 5 Ma, corresponding to the development of Fault III. Faults I and II rotate to lower angles and isotopic age data around 2 Ma represent a final shear on Fault I, now known as the Alaşehir detachment (Figure 6). The different isotopic ages obtained from the Alaşehir detachment (formerly Fault I) can be well explained by the rolling hinge mechanism in the Alaşehir graben. These data also support and explain the 3D model for the formation of the Horzum Turtleback surface.

4. A 3D model for the formation of the Horzum Turtleback in the Alaşehir graben

The Horzum Turtleback is located on the Alaşehir detachment. It has been defined by Çemen et al. (2000, 2005) and compared with its equivalents in the Basin and Range, but no mechanism for its development has been suggested.

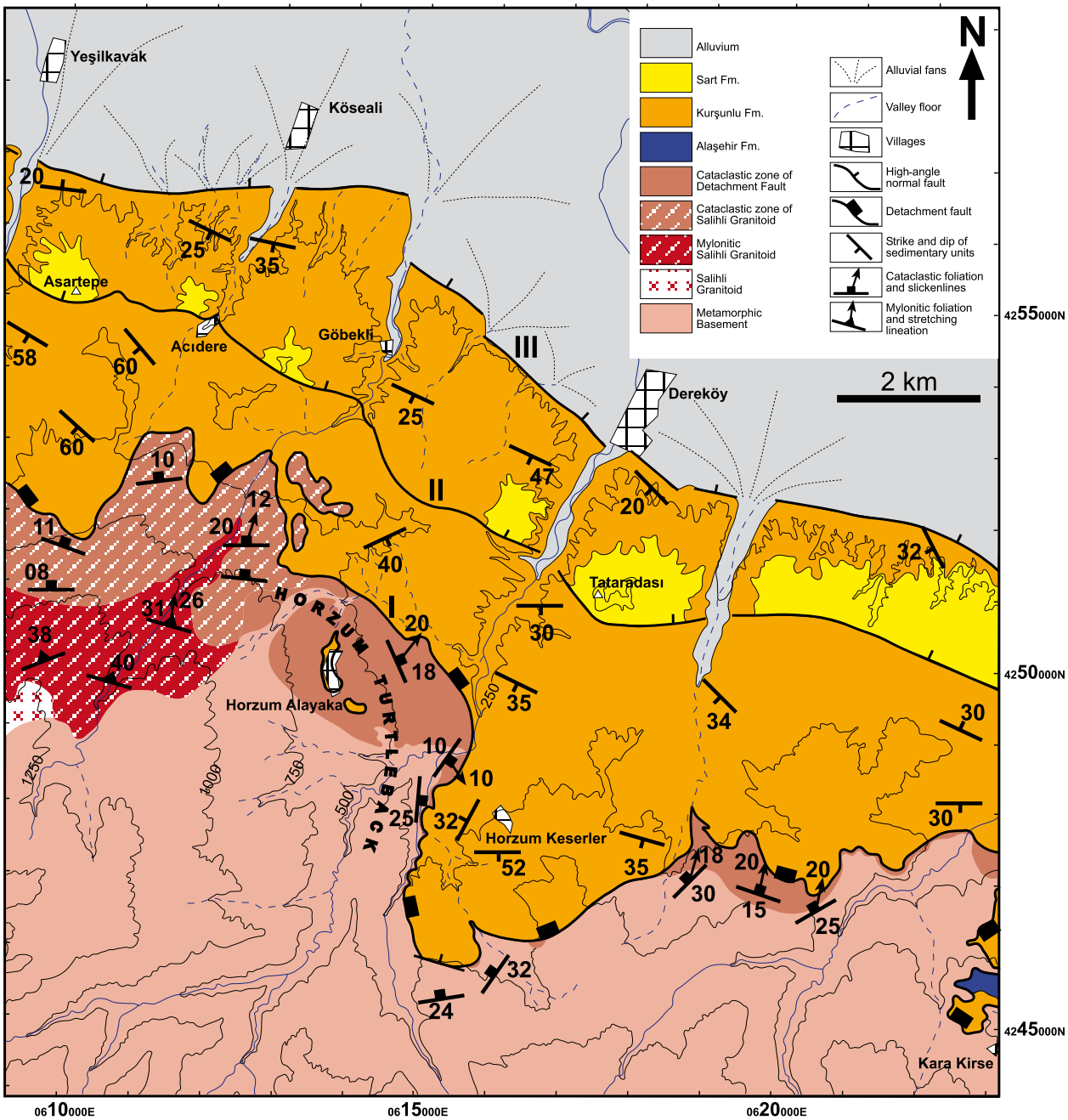

Figure 4. Geological map of the Horzum Turtleback (after Seyitoğlu et al., 2000, 2002; Sözbilir, 2001; Işık et al., 2003; Çemen et al., 2005; Öner and Dilek, 2011).

The combination of knowledge about the sedimentary basin development in the extensional tectonic regimes, and about the Alaşehir type rolling hinge mechanism and synextensional granitoid intrusion plus isotopic age data ranging between 21.7 ± 4.5 Ma and 1.75 ± 0.62 Ma published previously (Table), gives us an excellent opportunity to suggest a 3D model for this turtleback formation (Figures 7 and 8).

Extensional basins have 3 developing stages: 1) a fault initiation stage, 2) an interaction and linkage stage, and 3) a through-going fault zone stage (Gawthorpe and Leeder, 2000). In the Alaşehir graben, at the fault initiation stage, north-dipping high-angle normal faults were separated with a relay ramp (Seyitoğlu et al., 2002, p. 22), and in their hanging wall the first sedimentary unit was accumulating in 2 subbasins, which are obviously seen in gravity (Akçığ,

Table. Previously published isotopic age data from the Alaşehir detachment.

Map #	Sample no.	Latitude (°N)	Longitude (°E)	Age (Ma)	Error (±Ma)	Method	Reference
1	T70	38.404920	28.236000	1.87	0.36	AFT	
1	T70	38.404920	28.236000	5.19	0.28	ZFT	
2	T20	38.441100	28.067000	1.75	0.62	AFT	
3	T11	38.336030	28.071000	7.90	1.75	AFT	Gessner et al. (2001)
4	T14	38.319650	28.101000	3.73	0.61	AFT	
5	T15	38.319650	28.103000	6.08	0.83	AFT	
6	T16	38.336570	28.102000	8.74	2.67	AFT	
7	2	38.432972	28.091633	7.00	1.00	$^{40}Ar/^{39}Ar$	Lips et al. (2001)
8	01-88/9-1	38.320985	28.501796	17.00	5.00	Th-Pb	Catlos and Çemen (2005)
8	01-88/3-1	38.320985	28.501796	4.5	1.00	Th-Pb	
9	93T55	38.387500	28.254900	15.00	0.30	^{206}Pb-^{238}U	Glodny and Hetzel (2007)
10	93T103	38.386800	27.688700	16.10	0.20	^{207}Pb-^{235}U	
11	CC20-m6_2	38.406667	28.195278	21.70	4.50	Th-Pb	
11	CC20-m5_1	38.406667	28.195278	18.60	4.50	Th-Pb	
11	CC20-m2a_1	38.406667	28.195278	18.30	1.80	Th-Pb	
11	CC20-m6_1	38.406667	28.195278	16.00	1.60	Th-Pb	
11	CC20-m2b_1	38.406667	28.195278	13.00	1.10	Th-Pb	
11	CC20-m6_3	38.406667	28.195278	11.90	2.50	Th-Pb	
11	CC20-m3_1	38.406667	28.195278	11.00	2.60	Th-Pb	
11	CC20-m1_1	38.406667	28.195278	9.60	1.60	Th-Pb	
12	EB06-m2_1	38.382917	27.675611	15.50	1.20	Th-Pb	
12	EB06-m2_2	38.382917	27.675611	15.40	1.30	Th-Pb	
12	EB06-m4_1	38.382917	27.675611	15.10	1.00	Th-Pb	
13	EB08A-m1_1	38.382167	27.661306	15.00	1.40	Th-Pb	
13	EB08A-m1_2	38.382167	27.661306	13.90	1.00	Th-Pb	
13	EB08A-m2_1	38.382167	27.661306	14.00	0.80	Th-Pb	
13	EB08A-m3_1	38.382167	27.661306	12.20	1.40	Th-Pb	
13	EB08A-m4_1	38.382167	27.661306	14.30	0.80	Th-Pb	
13	EB08A-m4_2	38.382167	27.661306	11.50	0.80	Th-Pb	Catlos et al. (2010)
13	EB08B-m1_1	38.382167	27.661306	15.30	1.30	Th-Pb	
13	EB08B-m2_2	38.382167	27.661306	15.80	1.30	Th-Pb	
13	EB08B-m2_1	38.382167	27.661306	15.40	1.00	Th-Pb	
13	EB08B-m3_1	38.382167	27.661306	14.30	0.70	Th-Pb	
14	EB09A-m3a_2	38.381972	27.661528	19.20	5.10	Th-Pb	
14	EB09A-m1_1	38.381972	27.661528	16.80	1.10	Th-Pb	
14	EB09A-m4a_1	38.381972	27.661528	16.70	1.60	Th-Pb	
14	EB09A-m2b_1	38.381972	27.661528	16.10	1.40	Th-Pb	
14	EB09A-m3b_1	38.381972	27.661528	15.00	0.80	Th-Pb	
14	EB09A-m4b_1	38.381972	27.661528	14.90	1.20	Th-Pb	
14	EB09A-m3a_1	38.381972	27.661528	13.80	0.90	Th-Pb	
14	EB09A-m2a_1	38.381972	27.661528	13.20	0.80	Th-Pb	
14	EB09B-m2d_4	38.381972	27.661528	16.30	1.30	Th-Pb	
14	EB09B-m2c_1	38.381972	27.661528	15.70	1.30	Th-Pb	
14	EB09B-m2b_2	38.381972	27.661528	14.90	1.20	Th-Pb	
14	EB09B-m2a_3	38.381972	27.661528	14.60	4.20	Th-Pb	
14	EB09B-m1_1	38.381972	27.661528	14.10	1.00	Th-Pb	

Table. (Continued).

15	10JTB02	38.400500	28.223600	2.50	0.10	AHe	
15	10JTB02	38.400500	28.223600	2.00	0.10	ZHe	
15	10JTB02	38.400500	28.223600	2.60	1.30	AFT	
15	10JTB02	38.400500	28.223600	6.40	0.90	ZFT	
16	11M2	38.380400	28.182600	2.50	0.10	AHe	
17	11M3	38.381200	28.185000	2.00	0.20	AHe	
17	11M3	38.381200	28.185000	3.30	0.30	ZHe	
18	11M4	38.377500	28.180600	8.20	0.30	AHe	
19	11M5	38.396300	28.189800	1.70	0.20	AHe	
19	11M5	38.396300	28.189800	3.60	0.20	ZHe	
20	11M6	38.407300	28.196800	1.90	0.20	AHe	
20	11M6	38.407300	28.196800	2.20	0.10	ZHe	Buscher et al. (2013)
21	11M8	38.420500	28.207400	3.00	1.80	AHe	
21	11M8	38.420500	28.207400	18.40	1.30	ZHe	
22	11M11	38.298700	28.169300	2.60	2.60	AHe	
22	11M11	38.298700	28.169300	9.70	0.90	ZHe	
23	11M12	38.338800	28.100900	5.70	1.70	AHe	
24	11M13	38.366700	28.180300	2.10	0.03	AHe	
24	11M13	38.366700	28.180300	3.90	0.40	ZHe	
24	11M13	38.366700	28.180300	2.30	1.70	AFT	
25	11M14	38.332600	28.161000	3.50	1.50	AHe	
25	11M14	38.332600	28.161000	6.40	1.20	ZHe	
26	11M15	38.311900	28.167000	3.70	0.40	AHe	
26	11M15	38.311900	28.167000	8.10	1.30	ZHe	
27	10Me13	38.336767	28.411167	10.60	0.30	K-Ar	
28	10Me09	38.345050	28.406300	9.20	0.30	K-Ar	
28	10Me10	38.345050	28.406300	3.70	0.20	K-Ar	Hetzel et al. (2013)
28	10Me10	38.345050	28.406300	3.40	0.10	K-Ar	
28	10Me10	38.345050	28.406300	4.00	0.20	K-Ar	
28	10Me10	38.345050	28.406300	4.00	0.20	K-Ar	

1988; Ateş et al., 1999) and seismic reflection data (Çiftçi and Bozkurt, 2010, p. 865) (Figures 7a and 8a). In the interaction and linkage stage, the subbasins acted as a single basin in the hanging wall of Fault I (Figures 7b and 8b). At the midcrust, synextensional Salihli granitoid intruded to the ductile shear zone of Fault I (Hetzel et al., 1995; Işık et al., 2003; Öner et al., 2010) (Figure 8c). In the through-going fault zone stage, the development of Fault II in the Pliocene led Fault I to rotate at lower angles and this was enhanced by the formation of Fault III. Finally, Fault I became a low-angle detachment fault and the former relay ramp zone transformed into the turtleback surface with the help of the synextensional granitoid (Figures 7c, 7d, and 8d).

5. Morphotectonic features of the Horzum turtleback

Examination of the drainage basins as a morphotectonic study shows that the drainage basins around the study area have an approximately NE-SW elongated elliptical shape except for the Horzum Drainage Basin (HDB) (Figure 9). The HDB, where the Horzum Turtleback is located, covers a larger area than the adjacent drainage basins and contains the deepest valley floor in front of the detachment fault, as shown on the fault parallel cross-section (Figures 9 and 10a). In the turtleback surface, the drainage system adjusts itself to the new position and changes its orientation (Figure 9). This orientation changing also documents a continuous semidome-shaped exhumation of the fault surface. The changing dip of the fault surface creates

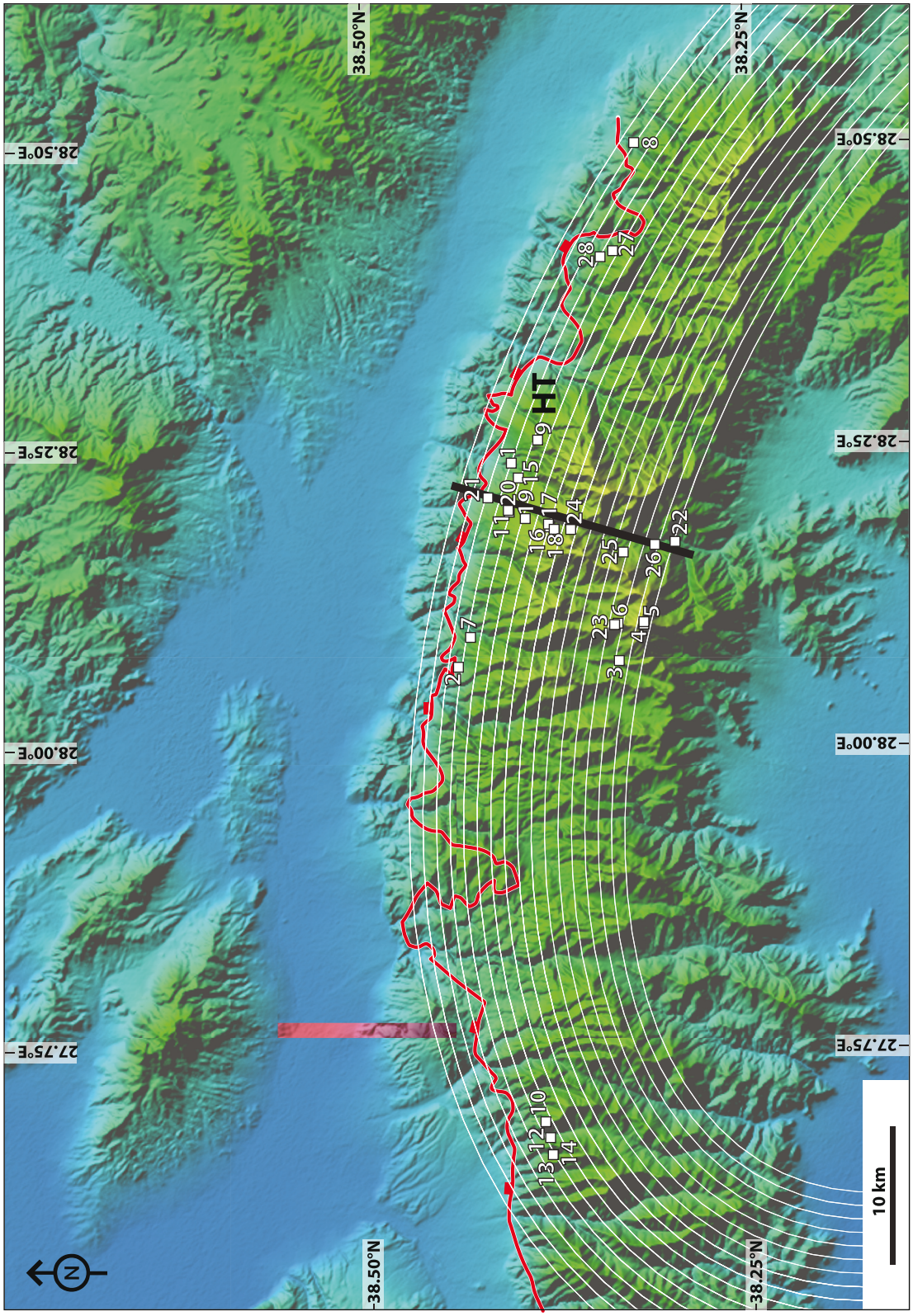

Figure 5. The map view of all available isotopic dating on the Alaşehir detachment. See the Table for references. Elliptical trajectories are used to plot sample locations on black cross-section line. See Figure 6 for the cross-section. HT: Horzum Turtleback. Red line represents the trace of Alaşehir detachment.

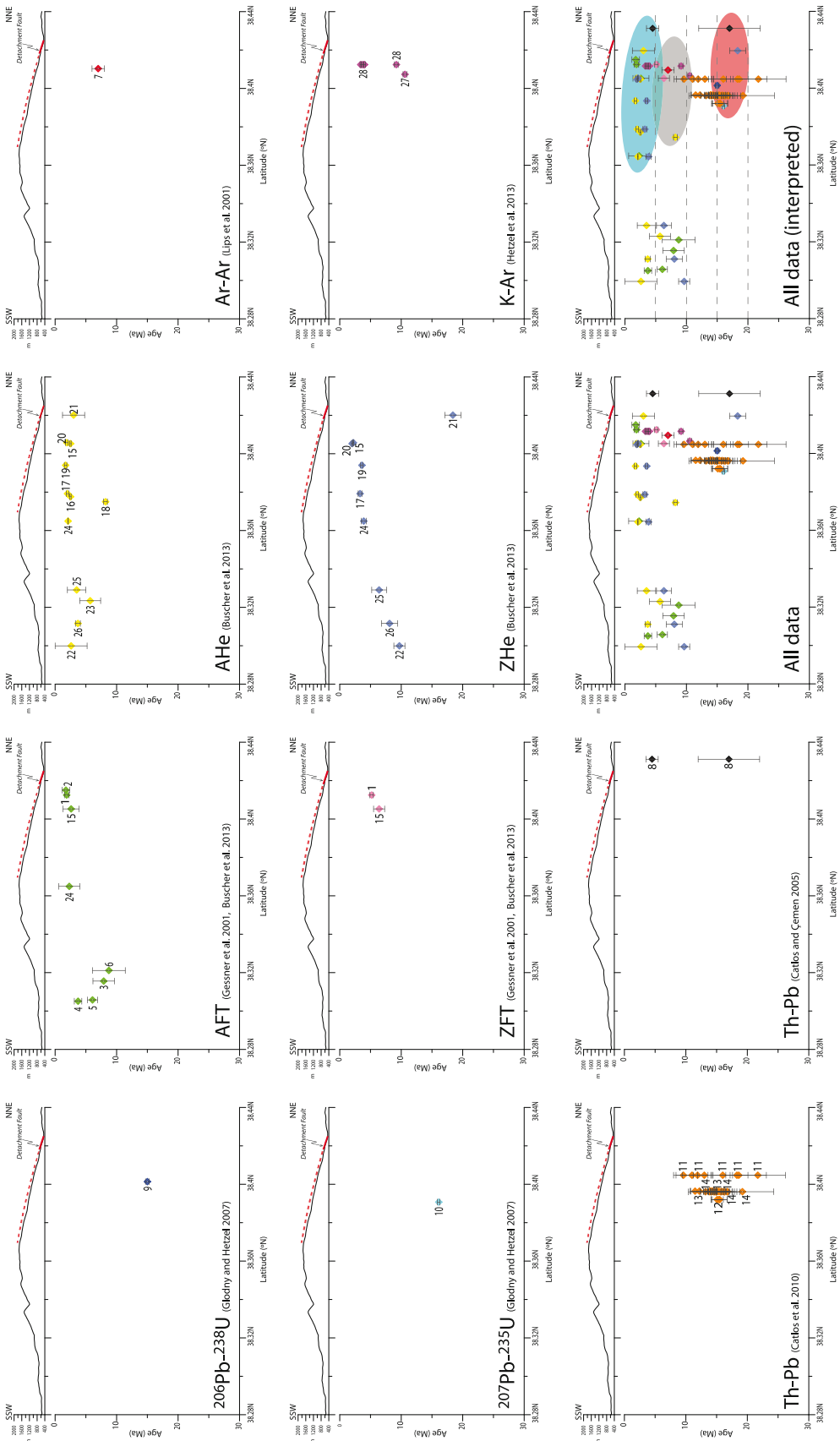

Figure 6. The cross-sectional view of all available data of isotopic dating on the Alaşehir detachment. For details, see the Table. See Figure 5 for the location of cross-section line and data.

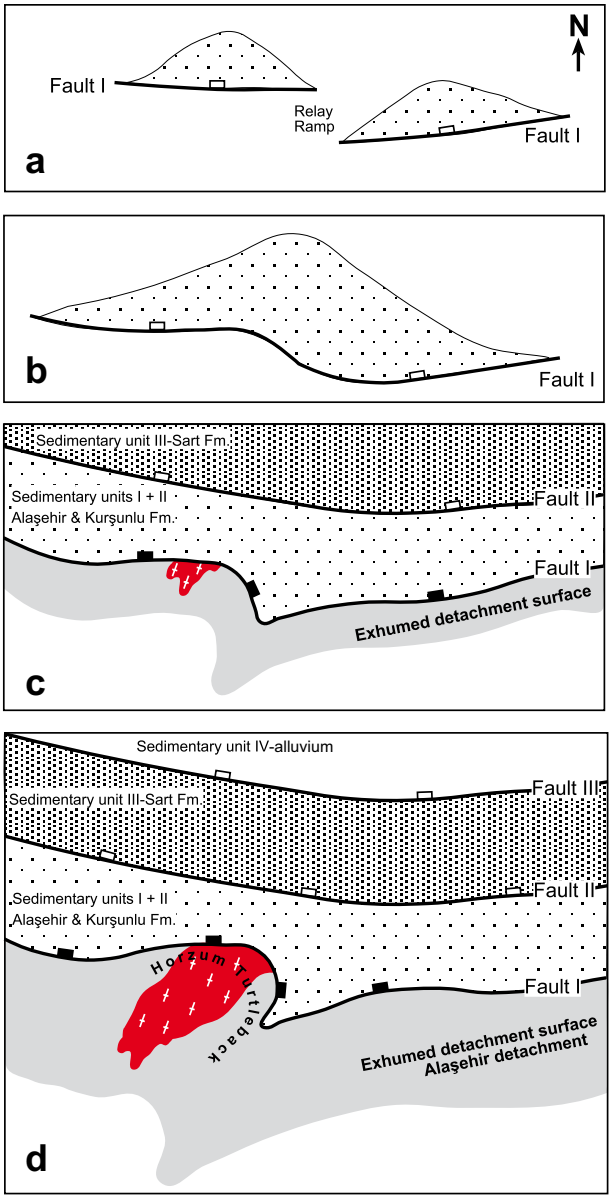

Figure 7. a–d) Schematic map view of turtleback development in the Alaşehir graben. See text for explanation.

asymmetrical valley slopes along the reoriented drainage, which is documented by the asymmetry factor (AF) (Figure 9) evaluating tectonic tilting (Hare and Gardner, 1985; Cox, 1994; Keller and Pinter, 2002). It is clearly observed from the cross-section nearly perpendicular to the fault surface that at the northeast part of the Horzum Turtleback, no distinct drainage is developed because of a recently exposed fault surface; further to the south, however, a well-established drainage system can be observed (Figure 10b).

6. Discussion

The formation mechanism of turtleback surfaces is part of a discussion associated with the amount of crustal extension in the Basin and Range Province of the western United States. Some researchers suggest that the turtleback formation is related to faults with high-angle origins requiring low to moderate amounts of extension for the Basin and Range (Wright et al., 1974; Miller, 1991). Others evaluate the turtleback surfaces as part of a regional detachment faulting, and therefore a high amount of extension is possible for the region (Steward, 1983; Wernicke et al., 1988).

In western Turkey, the Horzum Turtleback is related to high-angle origin faults that require moderate extension, but this situation does not exclude a high amount of extension in the region because it is widely agreed that the formation of the Alaşehir and Büyük Menderes grabens is related to the second-stage exhumation of the central Menderes massif by symmetrical core complex formation (Gessner et al., 2001; Seyitoğlu et al., 2002; Ring et al., 2003; Seyitoğlu and Işık, 2009). The main exhumation of the Menderes massif requiring a high amount of extension occurred earlier in the first stage by asymmetrical core complex formation in which the Datça-Kale main breakaway fault and its northern continuation, the Simav detachment fault, played an important role (Seyitoğlu et al., 2004). For this reason, the mechanism of the turtleback formation in western Turkey presented in this paper has no assignment to determine the amount of extension in the region. Moreover, the Horzum Turtleback cannot be attributed to the first-stage asymmetric core complex formation having constant top to NE sense of shear because the Horzum Turtleback shows fan-style slickenline distribution ranging from the NE to SE on its surface (Figure 4). This feature also differentiates the Horzum Turtleback from the simple corrugations of the Alaşehir detachment surface.

The Horzum Turtleback of western Turkey has a relatively simple geological setting when compared to the Death Valley turtlebacks because in the Alaşehir graben no major strike-slip system is documented. However, researchers in the Black Mountain area have to consider the influence of the strike-slip faulting on the formation mechanism of turtleback surfaces. A recently published paper by Norton (2011) suggests a close link between strike-slip systems and the Death Valley turtleback surfaces. Holm et al. (1993) documented 50°–80° clockwise vertical axis rotations that are considered to be due to right lateral strike-slip system. If the 50°–80° clockwise rotation reported by Holm et al. (1993) is reconstructed in the Black Mountains (Figure 11a), it could be speculated that the original locations of the Badwater, Copper Canyon, and Mormon Point turtlebacks are on the relay ramps of

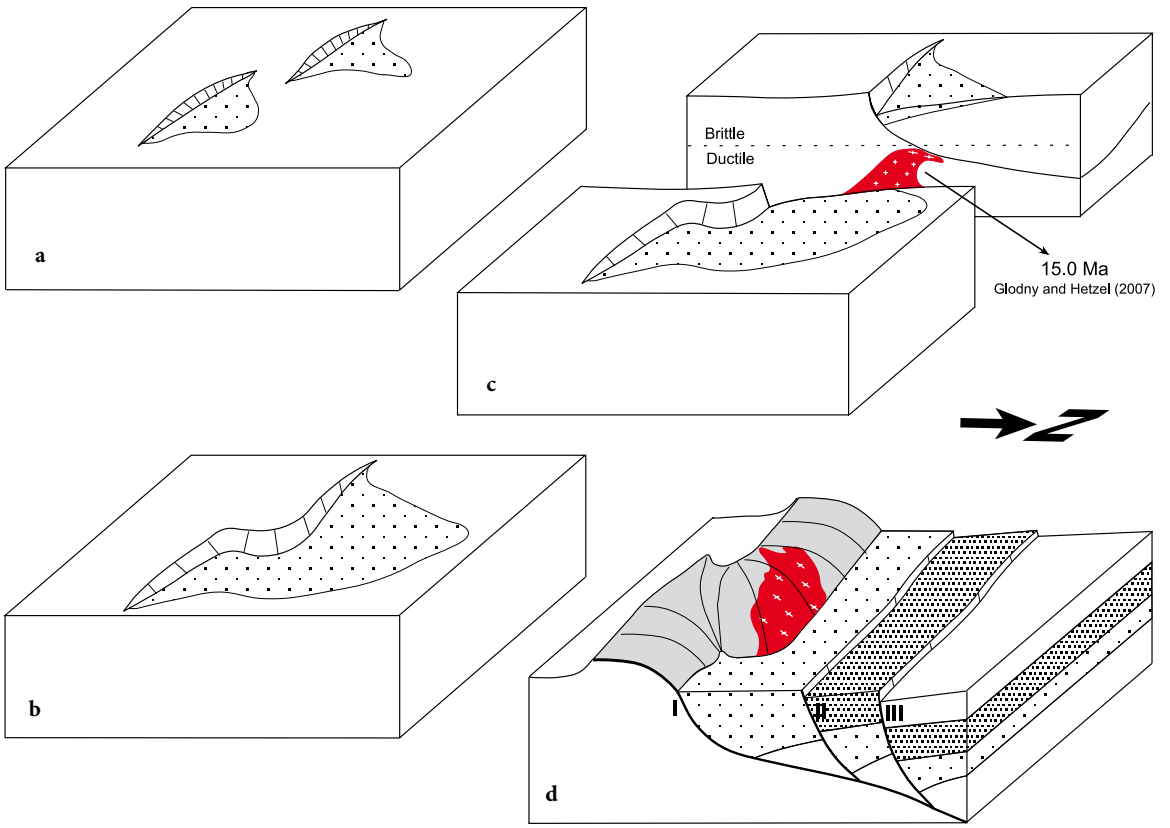

Figure 8. a–d) Block diagrams of turtleback development in the Alaşehir graben. See text for explanation.

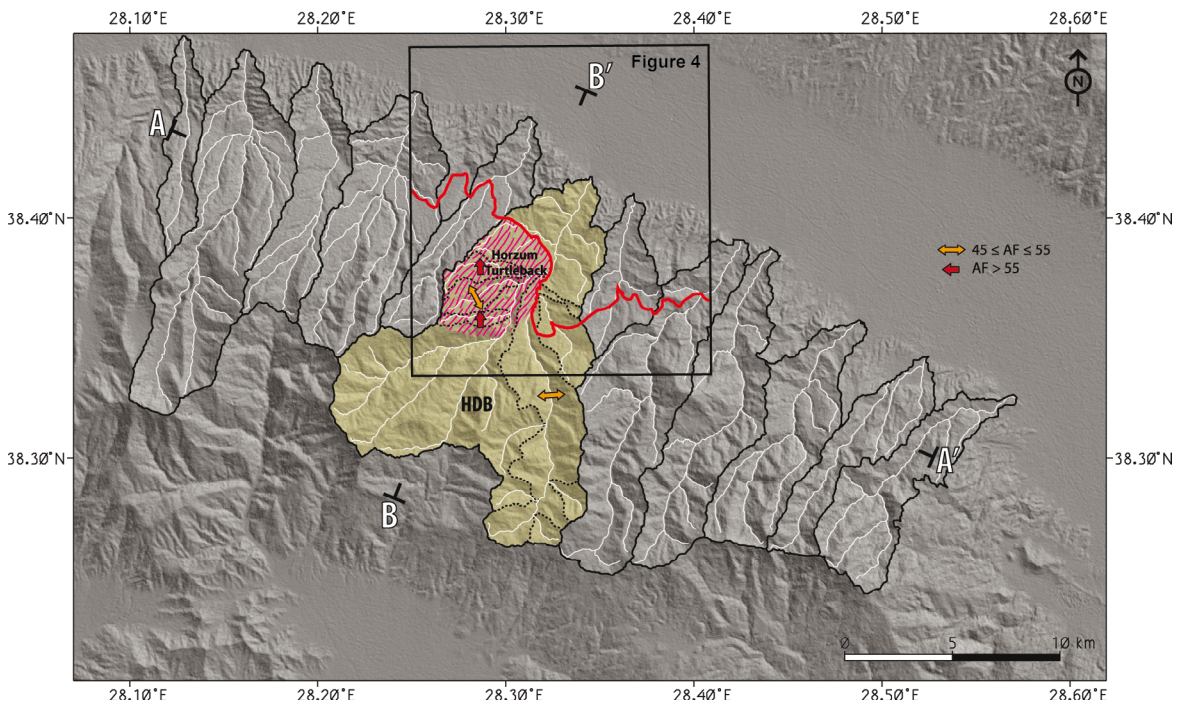

Figure 9. Drainage pattern of the Horzum Turtleback and surroundings. HDB: Horzum drainage basin. AF: Asymmetry factor detects tectonic tilting; AF = 100 (A_r / A_t), where A_r is the drainage area on the downstream right of the main drainage line and A_t is the total area of the drainage basin. Values of AF greater or less than 50 indicate tilting (Hare and Gardner, 1985; Cox, 1994; Keller and Pinter, 2002).

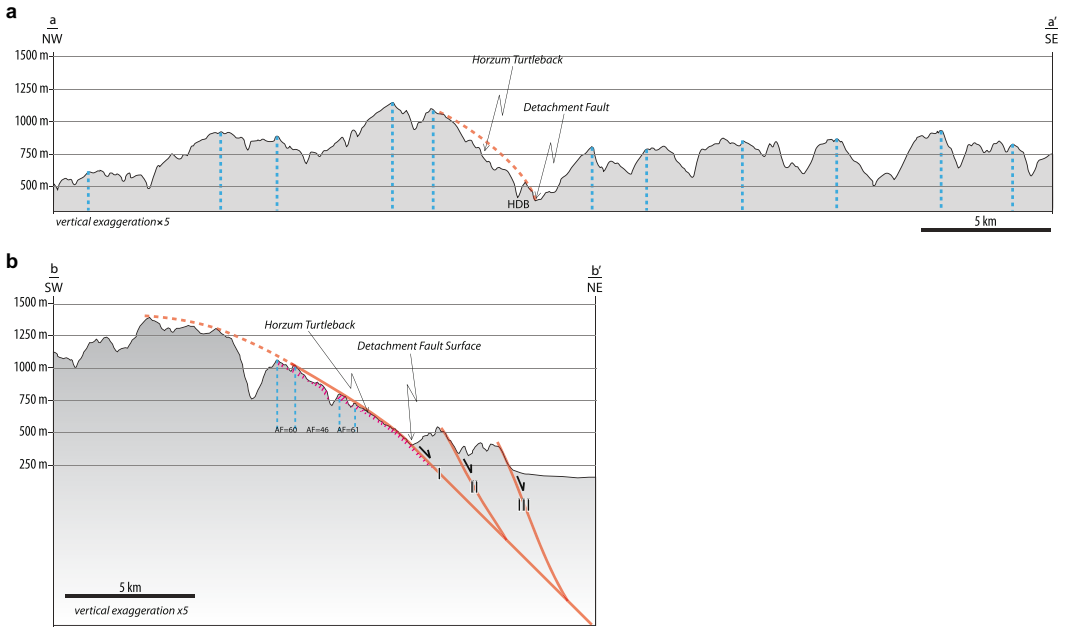

Figure 10. a) Topographical cross-section parallel to the graben axis. **b)** Topographical cross-section normal to the graben axis. Data for the underground position of faults are from Figures 3e and 3f. For location, see Figure 9.

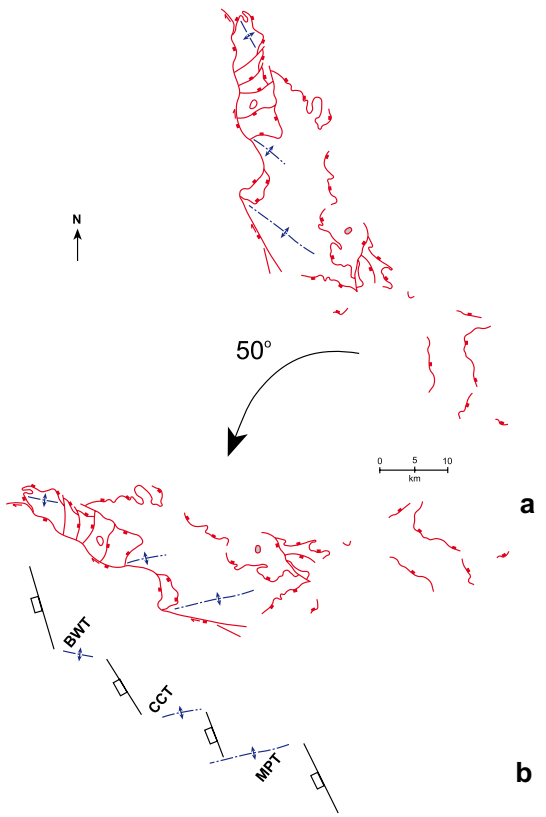

Figure 11. a) Reconstruction of the clockwise rotation in the Black Mountains (after Holm et al., 1993). **b)** Hypothetical positions of the Death Valley turtlebacks at the beginning of extensional basin formation. BWT: Badwater Turtleback, CCT: Copper Canyon Turtleback, MPT: Mormon Point Turtleback.

NNW-trending, WSW-dipping normal faults (Figure 11b), which is an interestingly similar position to that involved in the suggested mechanism of the Horzum Turtleback.

7. Conclusion

The Horzum Turtleback of the Alaşehir graben teaches us that there are 3 essential elements in the formation of turtleback surfaces: 1) the rolling hinge mechanism on normal faults, in which an initial normal fault is also active after forming second and third normal faults on its hanging wall; 2) a relay ramp between the segments of the initial normal fault; and 3) synextensional intrusion on the shear zone of the initial normal fault at midcrustal level. To create turtleback surfaces there is no need for a strike-slip setting as previously suggested by some researchers in the Basin and Range Province (Wright et al., 1974; Norton, 2011). After reconstruction of a clockwise rotation (Holm et al., 1993) in Death Valley, it is interesting to see that the original positions of the Badwater, Copper Canyon, and Mormon Point turtlebacks are located on the possible relay ramps between the normal fault segments.

Acknowledgments

The first author wishes to thank Mark Brandon for discussions on several structural problems including turtleback surfaces and to acknowledge the great help provided by the library facilities of Yale University during his sabbatical leave in 2011–2012. The editorial handling of Osman Candan and constructive comments of Aral Okay and 2 anonymous referees are greatly appreciated.

References

Akçığ Z (1988). Analysis of the tectonic problems of western Anatolia with the gravity data. Geol Bull Turkey 31: 63–70 (article in Turkish with an abstract in English).

Ateş A, Kearey P, Tufan S (1999). New gravity and magnetic anomaly maps of Turkey. Geophys J Int 136: 499–502.

Bozkurt E, Park RG (1994). Southern Menderes massif: an incipient metamorphic core complex in western Anatolia, Turkey. J Geol Soc London 151: 213–216.

Bozkurt E, Sözbilir H (2004). Tectonic evolution of the Gediz Graben: field evidence for an episodic, two-stage extension in western Turkey. Geol Mag 141: 63–79.

Buck WR (1988). Flexural rotation of normal faults. Tectonics 7: 959–973.

Buscher JT, Hampel A, Hetzel R, Dunkl I, Glotzbach C, Struffert A, Akal C, Ratz M (2013). Quantifying rates of detachment faulting and erosion in the central Menderes massif (western Turkey) by thermochronology and cosmogenic 10Be. J Geol Soc London 170: 669–683.

Candan O, Koralay OE, Akal C, Kaya O, Oberhansli R, Dora OÖ, Konak N, Chen F (2011). Supra-Pan-African unconformity between core and cover series of the Menderes massif/Turkey and its geological implications. Precambrian Res 184: 1–23.

Catlos EJ, Baker C, Sorensen SS, Çemen İ, Hançer M (2010). Geochemistry, geochronology and cathodoluminescence imagery of the Salihli and Turgutlu granites (Central Menderes Massif, western Turkey): Implications for Aegean tectonics. Tectonophysics 488: 110–130.

Catlos EJ, Çemen I (2005). Monazite ages and the evolution of the Menderes massif, western Turkey. Int J Earth Sci 94: 204–217.

Çemen İ, Tekeli O, Seyitoğlu G (2000). Are the turtleback fault surfaces common structural elements of the strongly extended terranes? Geological Society of America Abstracts with Programs 32: A157–A158.

Çemen İ, Tekeli O, Seyitoğlu G, Işık V (2005). Are turtleback fault surfaces common structural elements of highly extended terranes? Earth-Sci Rev 73: 139–148.

Çiftçi NB, Bozkurt E (2010). Structural evolution of the Gediz Graben, SW Turkey: temporal and spatial variation of the graben basin. Basin Res 22: 846–873.

Cox RT (1994). Analysis of drainage-basin symmetry as a rapid technique to identify areas of possible Quaternary tilt-block tectonics: an example from the Mississippi embayment. Geol Soc Am Bull 106: 571–581.

Curry HD (1938). "Turtleback" fault surfaces in Death Valley, California. Geol Soc Am Bull 49: 1875.

Curry HD (1949). "Turtlebacks" of central Black Mountains, Death Valley, California. Geol Soc Am Bull 60: 1882.

Curry HD (1954). Turtlebacks in the central Black Mountains, Death Valley, California. California, Division of Mines and Geology Bulletin 170: 53–59.

Davis G (1980). Structural characteristics of metamorphic core complexes, southern Arizona. In: Crittenden MD Jr, Coney PJ, Davis GH, editors. Cordilleran Metamorphic Core Complexes. Geological Society of America Memoir 153. Boulder, CO, USA: Geological Society of America, pp. 35–78.

Demircioğlu D, Ecevitoğlu B, Seyitoğlu G (2010). Evidence of a rolling hinge mechanism in the seismic records of hydrocarbon-bearing Alaşehir graben, western Turkey. Petrol Geosci 16: 155–160.

Drewes HD (1959). Turtleback faults of Death Valley, California; A reinterpretation. Geol Soc Am Bull 70: 1497–1508.

Ediger V, Batı Z, Yazman M (1996). Paleopalynology of possible hydrocarbon source rocks of the Alaşehir - Turgutlu area in the Gediz graben (western Anatolia). Turkish Association of Petroleum Geologists Bulletin 8: 94–112.

Gawthorpe RL, Leeder MR (2000). Tectonosedimentary evolution of active extensional basins. Basin Res 12: 195–218.

Gessner K, Ring U, Johnson C, Hetzel R, Passchier CW, Güngör T (2001). An active bivergent rolling-hinge detachment system. Central Menderes metamorphic core complex in western Turkey. Geology 29: 611–614.

Glodny J, Hetzel R (2007). Precise U–Pb ages of syn-extensional Miocene intrusions in the central Menderes Massif, western Turkey. Geol Mag 144: 235–246.

Gürer ÖF, Sarıca-Filoreau N, Özburan M, Sangu E, Doğan B (2009). Progressive development of the Büyük Menderes Graben based on new data, western Turkey. Geol Mag 146: 652–673.

Hare PW, Gardner TW (1985). Geomorphic indicators of vertical neotectonism along converging plate margins, Nicoya Peninsula, Costa Rica. In: 15th Annual Binghamton Geomorphology Symposium Proceedings, September 1984. Crows Nest, Australia: Allen and Unwin Inc., pp. 75–104.

Hetzel R, Ring U, Akal C, Troesch M (1995). Miocene NNE-directed extensional unroofing in the Menderes massif, southwestern Turkey. J Geol Soc London 152: 639–654.

Hetzel R, Zwigmann H, Mulch A, Gessner K, Akal C, Hampel A, Güngör T, Petschick R, Mikes T, Wedin F (2013). Spatiotemporal evolution of brittle normal faulting and fluid infiltration in detachment fault systems: a case study from Menderes massif, western Turkey. Tectonics 32: 1–13.

Hill ML, Troxel BW (1966). Tectonics of Death Valley Region, California. Geol Soc Am Bull 77: 435–438.

Hinsbergen DJJ (2010). A key extensional metamorphic complex reviewed and restored: The Menderes Massif of western Turkey. Earth-Sci Rev 102: 60–76.

Holm DK, Fleck RJ, Lux DR (1994). The Death Valley turtlebacks reinterpreted as Miocene-Pliocene folds of a major detachment surface. J Geol 102: 718–727.

Holm DK, Geissman JW, Wernicke B (1993). Tilt and rotation of the footwall of a major normal fault system; paleomagnetism of the Black Mountains, Death Valley extended terrane, California. Geol Soc Am Bull 105: 1373–1387.

Holm DK, Snow JK, Lux DR (1992). Thermal and barometric constraints on the intrusive and unroofing history of the Black Mountains: implications for timing, initial dip, and kinematics of detachment faulting in the Death Valley region, California. Tectonics 11: 507–522.

Holm DK, Wernicke B (1990). Black Mountains crustal section, Death Valley extended terrain, California. Geology 18: 520–523.

Işık V, Seyitoğlu G, Çemen İ (2003). Ductile-brittle transition along the Alaşehir shear zone and its structural relationship with the Simav detachment, Menderes massif, western Turkey. Tectonophysics 374: 1–18.

Işık V, Tekeli O (2001). Late orogenic crustal extension in the northern Menderes massif (western Turkey): evidence for metamorphic core complex formation. Int J Earth Sci 89: 757–765.

Işık V, Tekeli O, Seyitoğlu G (2004). The 40Ar/39Ar age of extensional ductile deformation and granitoid intrusion in the northern Menderes core complex: implications for the initiation of extensional tectonics in western Turkey. J Asian Earth Sci 23: 555–566.

Keller EA, Pinter N (2002). Active Tectonics: Earthquakes, Uplift and Landscape. Upper Saddle River, NJ, USA: Prentice Hall.

Koçyiğit A, Yusufoğlu H, Bozkurt E (1999). Evidence from the Gediz graben for episodic two-stage extension in western Turkey. J Geol Soc London 156: 605–616.

Lips ALW, Cassard D, Sözbilir H, Yılmaz H (2001). Multistage exhumation of the Menderes massif, western Anatolia (Turkey). Int J Earth Sci 89: 781–792.

Miller MB, Pavlis TL (2005). The Black Mountains turtlebacks: Rosetta stones of Death Valley tectonics. Earth-Sci Rev 73: 115–138.

Miller MG (1991). High-angle origin of the currently low-angle Badwater Turtleback fault, Death Valley, California. Geology 19: 372–375.

Miller MG, Prave AR (2002). Rolling hinge or fixed basin?: a test of continental extensional models in Death Valley, California, United States. Geology 30: 847–850.

Norton I (2011). Two-stage formation of Death Valley. Geosphere 7: 171–182.

Öner Z, Dilek Y (2011). Supradetachment basin evolution during continental extension: the Aegean province of western Anatolia, Turkey. Geol Soc Am Bull 123: 2115–2141.

Öner Z, Dilek Y, Kadıoğlu YK (2010). Geology and geochemistry of the synextensional Salihli granitoid in the Menderes core complex, western Anatolia, Turkey. Int Geol Rev 52: 336–368.

Purvis M, Robertson AHF (2005). Sedimentation of the Neogene–Recent Alaşehir (Gediz) continental graben system used to test alternative tectonic models for western (Aegean) Turkey. Sedimentary Geology 173: 373–408.

Rehrig WA, Reynolds SJ (1980). Geologic and geochronologic reconnaissance of a northwest-trending zone of metamorphic core complexes in southern and western Arizona. In: Crittenden MD Jr, Coney PJ, Davis GH, editors. Cordilleran Metamorphic Core Complexes. Geological Society of America Memoir 153. Boulder, CO, USA: Geological Society of America, pp. 131–157.

Ring U, Johnson C, Hetzel R, Gessner K (2003). Tectonic denudation of a late Cretaceous-Tertiary collisional belt: regionally symmetric cooling patterns and their relation to extensional faults in the Anatolide belt of western Turkey. Geol Mag 140: 421–441.

Şen Ş, Seyitoğlu G (2009). Magnetostratigraphy of early-middle Miocene deposits from E-W trending Alaşehir and Büyük Menderes grabens in western Turkey, and its tectonic implications. In: Van Hinsbergen DJJ, Edwards MA, Govers R, editors. Geodynamics of Collision and Collapse at the Africa-Arabia-Eurasia subduction zone. London, UK: Geological Society (London) Special Publication 311, pp. 321–342.

Şengör AMC, Bozkurt E (2013). Layer parallel shortening and related structures in zones undergoing active regional horizontal extension. Int J Earth Sci 102: 101–119.

Şengör AMC, Satır M, Akkök R (1984). Timing of tectonic events in the Menderes massif, western Turkey: implications for tectonic evolution and evidence for Pan-African basement in Turkey. Tectonics 3: 693–707.

Seyitoğlu G, Çemen İ, Tekeli O (2000). Extensional folding in the Alaşehir (Gediz) graben, western Turkey. J Geol Soc London 157: 1097–1100.

Seyitoğlu G, Işık V (2009). Meaning of the Küçük Menderes graben in the tectonic framework of the central Menderes metamorphic core complex (western Turkey). Geol Acta 7: 323–331.

Seyitoğlu G, Işık V, Çemen İ (2004). Complete Tertiary exhumation history of the Menderes massif, western Turkey: an alternative working hypothesis. Terra Nova 16: 358–364.

Seyitoğlu G, Scott BC (1996). Age of Alaşehir graben (west Turkey) and its tectonic implications. Geol J 31: 1–11.

Seyitoğlu G, Şen Ş (1998). The contribution of first magnetostratigraphical data from E-W trending grabens fill to the style of late Cenozoic extensional tectonics in western Turkey. In: 3rd International Turkish Geology Symposium, Abstracts, Ankara, Turkey, p. 188.

Seyitoğlu G, Tekeli O, Çemen İ, Şen Ş, Işık V (2002). The role of the flexural rotation/rolling hinge model in the tectonic evolution of the Alaşehir graben, western Turkey. Geol Mag 139: 15–26.

Sözbilir H (2001). Extensional tectonics and the geometry of related macroscopic structures: field evidence from the Gediz detachment, western Turkey. Turk J Earth Sci 10: 51–67.

Stewart JH (1983). Extensional tectonics in the Death Valley area, California; Transport of the Panamint Range structural block 80 km northwestward. Geology 11: 153–157.

ten Veen JH, Boulton SJ, Alçiçek MC (2009). From palaeotectonics to neotectonics in the Neotethys realm: The importance of kinematic decoupling and inherited structural grain in SW Anatolia (Turkey). Tectonophysics 437: 261–281.

Wernicke B (1981). Low-angle normal faults in the Basin & Range province: nappe tectonics in an extending orogen. Nature 291: 645–648.

Wernicke B, Axen GJ (1988). On the role of isostasy in the evolution of normal fault systems. Geology 16: 848–851.

Wernicke B, Axen G, Snow JK (1988). Basin and Range extensional tectonics at the latitude of Las Vegas, Nevada. Geol Soc Am Bull 100: 1738–1757.

Wright LA, Otten J, Troxel BW (1974). Turtleback fault surfaces of Death Valley viewed as phenomena of extension. Geology 2: 53–54.

Yılmaz M, Gelişli K (2003). Stratigraphic–structural interpretation and hydrocarbon potential of the Alaşehir Graben, Western Turkey. Petrol Geosci 9: 277–282.

Yılmaz Y, Genç SC, Gürer F, Bozcu M, Yılmaz K, Karacık Z, Altunkaynak S, Elmas A (2000). When did the western Anatolian grabens begin to develop? In: Bozkurt E, Winchester JA, Piper JDA, editors. Tectonics and Magmatism in Turkey and the Surrounding Area. London, UK: Geological Society (London) Special Publication 173, pp. 353–384.